AQUA
Water Infrastructure, Ecosystems and Society

IWA PUBLISHING

 AQUA — Water Infrastructure, Ecosystems and Society Vol 72 No 11, 2035 doi: 10.2166/aqua.2023.117

Phyto-assisted synthesis of magnetic $NiFe_2O_4$ nanocomposite using the *Pulicaria gnaphalodes* methanolic extract for the efficient removal of an antibiotic from the aqueous solution: a study of equilibrium, kinetics, isotherms, and thermodynamics

Elham Derakhshani[a], Ali Naghizadeh[b,*] and Sobhan Mortazavi-Derazkola[b]

[a] Student Research Committee, Birjand University of Medical Sciences, Birjand, Iran
[b] Medical Toxicology and Drug Abuse Research Center (MTDRC), Birjand University of Medical Sciences (BUMS), Birjand, Iran
*Corresponding author. E-mail: al.naghizadeh@yahoo.com

ABSTRACT

In this research, the magnetic $NiFe_2O_4$ nanocomposite was synthesized using *Pulicaria gnaphalodes* methanolic extract and applied to remove penicillin G from aqueous solutions. The results of field emission scanning electron microscopy, X-ray powder diffraction, Fourier transform infrared, Vibrating-Sample Magnetometer (VSM), and energy-dispersive spectroscopy-mapping analyses showed that this nanocomposite was well synthesized with a size of approximately 50–70 nm. The maximum adsorption capacity of the magnetic $NiFe_2O_4$ nanocomposite was 22.95 mg/g under optimal conditions. In addition, the experimental data of penicillin G adsorption by the magnetic $NiFe_2O_4$ nanocomposite showed that ΔH and ΔS values were positive and ΔG was negative and were following the Temkin isotherm model with $R^2 = 0.99$ and follows the pseudo-second-order kinetic model.

Key words: adsorption, isotherm, kinetic, nanocomposite, penicillin G, thermodynamic

HIGHLIGHTS

- The adsorption of penicillin G by $NiFe_2O_4$ was maximum in optimal conditions (pH = 3, nanocomposite dose: 0.3 g/L, penicillin G concentration: 30 g/L, contact time: 20 min, and time temperature: 313 K).
- The thermodynamic study of the adsorption process showed that the values of ΔH and ΔS are positive and ΔG is negative.
- Penicillin G adsorption by $NiFe_2O_4$ nanoparticles conforms to Temkin isotherm with $R^2 = 0.99$.

GRAPHICAL ABSTRACT

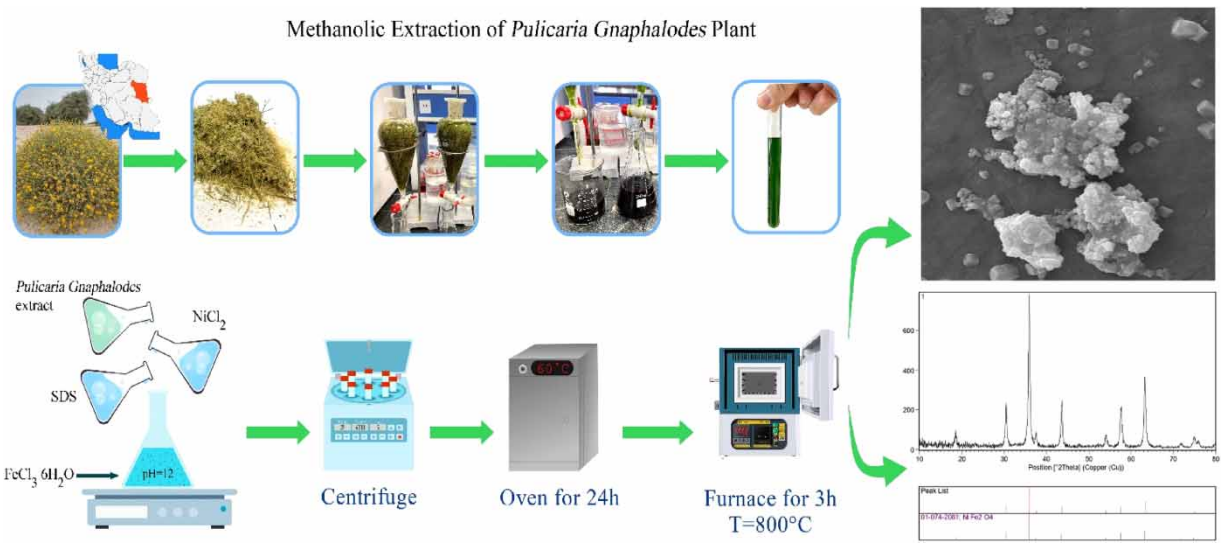

1. INTRODUCTION

Today, nanotechnology is one of the newest developing sciences and has wide applications in various fields such as medicine, agriculture, pharmaceuticals, aerospace, environment, and electronic industries (Naghizadeh *et al.* 2013a; Sinsinwar *et al.* 2018; Mortazavi-Derazkola *et al.* 2021a). Nanomaterials are very small particles that have nanodimensions from 1 to 100 nm. Since nanocomposites have a high surface-to-volume ratio, they have properties such as chemical stability, thermal conductivity, and high catalytic properties (Agarwal *et al.* 2017; Naghizadeh *et al.* 2017a). In recent years, magnetic nanomaterials, the most important of which are spinel ferrites with the general formula MFe_2O_4 (M = Ni, Fe, Cu, Co, Mn, etc.) due to their high removal capacity, reactivity to remove environmental pollutants, fast kinetics, efficiency isolation, and reusability, have received much attention from researchers (Teymourian *et al.* 2013; Zandipak & Sobhanardakani 2016). Nickel ferrite ($NiFe_2O_4$) has been widely studied as one of the most important magnetic nanocomposites due to its thermal stability and stable resistance. These magnetic nanocomposites have various applications such as gas sensors, catalysts, magnetic storage systems, photomagnetic materials, transformers, microwave devices, and magnetic temperature converters (Sivakumar *et al.* 2011a; Abu-Dief *et al.* 2016). Various physical and chemical methods, such as sol–gel processes (Fardood *et al.* 2017), hydrothermal (Li *et al.* 2010), co-precipitation (Sivakumar *et al.* 2011b), microemulsion (Hirai *et al.* 1999), and microwave synthesis (Bousquet-Berthelin *et al.* 2008), have been used for the synthesis of the nickel ferrite magnetic nanocomposite. In general, nanocomposite synthesis methods include physical, chemical, and biological methods (biosynthesis), of which biosynthesis of the metal nanocomposite is a possible alternative method for physical and chemical methods due to its compatibility with the environment, not use of toxic chemicals, cost-effectiveness, and less energy consumption (Iravani 2011; Hussain *et al.* 2016; Roy *et al.* 2017). Biosynthesis refers to the synthesis of nanocomposites through biological pathways such as plant extracts, enzymes, fungi, and bacteria. The use of plant extracts for the green synthesis of nanocomposites has received much attention from researchers due to their biological safety and cheapness (Rana *et al.* 2020; Derakhshani *et al.* 2023b). In recent years, the use of these nanocomposites in the removal of environmental pollutants, including antibiotics, is considered one of the newest methods of removing pollutants in the world. Penicillin G is one of the antibiotics that is widely used.

Today, large amounts of antibiotics have been identified that enter the human environment through pharmaceutical industry wastewater, hospital, and urban wastewater. An antibiotic is a substance that can kill microorganisms or inhibit their growth or metabolic activity (Dehghani *et al.* 2014; Choudhary *et al.* 2021). Antibiotics have been detected in very low concentrations (ppt) in surface and underground water sources and high concentrations (ppm) in hospital wastewater, and usually their concentration (ppb) in municipal wastewater is between these two ranges (Kümmerer 2009). Antibiotics are grouped into two categories: non-beta-lactam and beta-lactam, based on having a beta-lactam ring in their structure. Beta-lactam antibiotics are a large group of antibiotics that include penicillins, cephalosporins, monobactams, and carbapenems. Most beta-lactam antibiotics act by affecting the cell walls of bacteria and are active against many anaerobic, Gram-positive and Gram-negative organisms (Kamranifar *et al.* 2019a, 2019b). Penicillin G, which is produced from a fungus called *Penicillium chrysogenum*, is classified as an antibiotic with a beta-lactam ring. Due to its high production and its wide use in the treatment of syphilis, staphylococcal, and streptococcal infections, this drug is of great interest to health officials (Mohammadi & Sardar 2013). Antibiotics are lipophilic and stable compounds and can remain in the environment for a long time, so their presence is dangerous even in low concentrations. These compounds are very resistant to biological degradation and cause bacterial resistance; therefore, they are considered a threat to human health (Bound & Voulvoulis 2006; Xu *et al.* 2007). Common processes used in water and wastewater treatment are usually not capable of removing or destroying antibiotics, which is why researchers use physical treatment, chemical oxidation, and biological degradation to remove these contaminants from aquatic environments (Klavarioti *et al.* 2009; Le-Minh *et al.* 2010; El-Shafey *et al.* 2012). Among these methods, we can mention nanofiltration (Yang *et al.* 2018), photo-Fenton (Chaudhuri & Elmolla 2008), surface adsorption (Peng *et al.* 2019), photocatalytic destruction (Gad-Allah *et al.* 2011; Xekoukoulotakis *et al.* 2011), and coagulation (Choi *et al.* 2008). Some of these methods, despite having advantages, also have disadvantages that limit their use. For example, the advanced oxidation process is very expensive and complex and may produce undesirable oxidation by-products (Githinji *et al.* 2011; Wang *et al.* 2017). The use of membrane separation technologies such as nanofiltration may be problematic due to membrane fouling (Wang *et al.* 2017). Among these methods, adsorption is an effective method to remove various pollutants, that is simple, practical, and low-cost, and does not produce toxic by-products (Han *et al.* 2008). In the process of surface adsorption in aqueous solutions, the adsorbed materials that are in solution form accumulate on the surface of the absorbent solid material. In recent years, much attention has been paid to the synthesis of nanocomposites as adsorbents in water and

wastewater treatment (Akbari *et al.* 2019). In this research, the $NiFe_2O_4$ magnetic nanocomposite was used to remove penicillin G from aqueous solutions, and the effects of various parameters such as pH, penicillin G concentration, adsorbent dose, contact time, temperature and thermodynamic process, isotherm, and kinetics of the absorption process were investigated.

2. MATERIALS AND METHODS

2.1. Chemicals and reagents

In the present study, chemical materials such as iron(III) nitrate [$Fe(NO_3)_3{\cdot}9H_2O$], nickel nitrate [$NiCl_2{\cdot}6H_2O$], sodium hydroxide [NaOH], sodium dodecyl sulfate surfactant (SDS), hydrochloric acid [HCl], ethylene glycol [$C_2H_6O_2$], and sodium thiosulfate [$Na_2S_2O_3$] were obtained from Merck Company. Penicillin G was obtained from the Sigma Aldrich Company. It should be noted that all solutions were prepared freshly before the experiments.

2.2 Preparation of *Pulicaria gnaphalodes* extract

Pulicaria gnaphalodes plants were collected from all over South Khorasan, Birjand, Iran. First, fresh *P. gnaphalodes* was washed three times with water and then three times with deionized water. Then, the amount of dried powder was extracted with a methanol solution (percolation process; percolation is the process of slowly passing a liquid through a filter). The solvent was removed using a rotary vacuum evaporator (Hei zbad WB eoc, Germany).

2.3 Biosynthesis of the $NiFe_2O_4$ magnetic nanocomposite

The magnetic $NiFe_2O_4$ nanocomposite was prepared according to Shirzadi-Ahodashti *et al.*'s (2020) research. In a typical procedure, 5 g of iron nitrate hexahydrate ($Fe(NO_3)_3{\cdot}9H_2O$) was dissolved in 70 mL of deionized water under nitrogen gas conditions for 1 h. In a separate container, the SDS surfactant (with a molar ratio of 1:1 to iron salt) was dissolved in 30 mL of distilled water and with *P. gnaphalodes* extract added to iron salt. The reaction continued for 30 min under vigorous stirring at room temperature. Then, 1.47 g of nickel chloride salt ($NiCl_2{\cdot}6H_2O$) was added to the reaction solution. Finally, the pH of the reaction reached 12 by adding 2 M sodium hydroxide. After 2 h, the sediments obtained were washed and dried after centrifugation at room temperature for 24 h. The magnetic $NiFe_2O_4$ nanocomposite was obtained by calcination of the precipitations obtained at 600 °C for 3 h. The schematic of methanolic extraction and biosynthesis of magnetic $NiFe_2O_4$ nanocomposite is shown in Figure 1.

2.4 Characterization and analytical methods

X-ray powder diffraction (XRD) analysis was performed by using a Philips PW1800 X-ray diffractometer using nickel-filtered CuKα radiation ($\lambda = 0.154$ nm) at two angles from 10° to 80°. Field emission scanning electron microscopy (FESEM) spectra were done by using the TESCAN MIRAIII model, energy-dispersive X-ray spectroscopy (EDX) (TESCAN, MIRA III, Czech

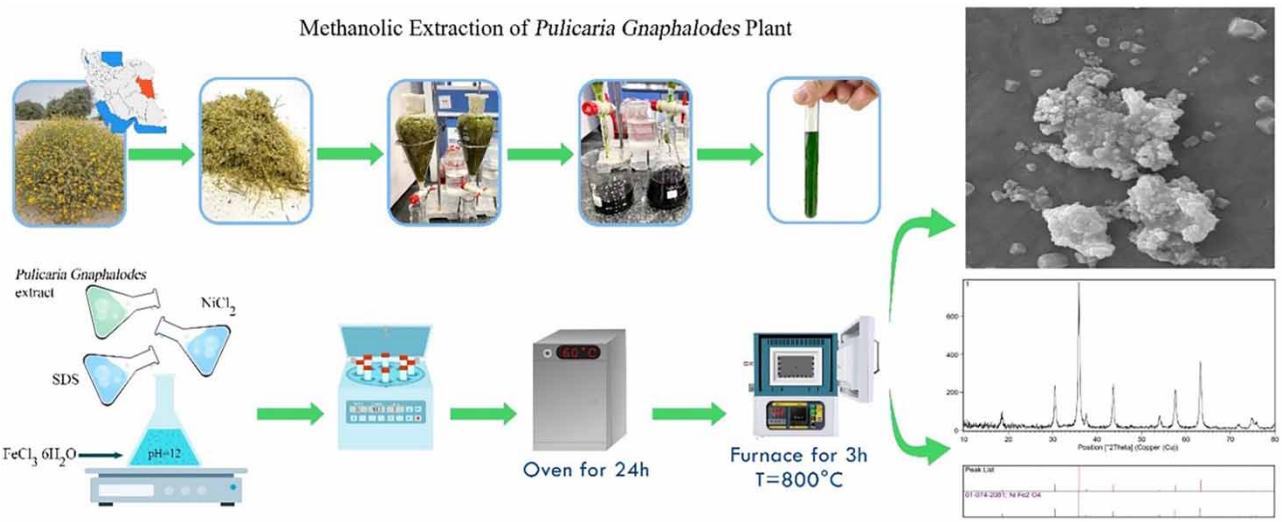

Figure 1 | Schematic of methanolic extraction and biosynthesis of the magnetic $NiFe_2O_4$ nanocomposite.

Republic), and Raman spectroscopy (Micro Raman Spectrometer, Avantes, Netherland). A Perkin–Elmer spectrum 100 Fourier transform infrared (FTIR) spectrometer was used for FTIR measurements.

2.5 Experimental setup

In this study, the effects of various parameters such as pH, dosage of magnetic $NiFe_2O_4$ nanocomposite, initial concentrations of penicillin G, contact times, and temperature on the removal rate of penicillin G from aqueous solutions were investigated. The methods of evaluating the effect of these variables are summarized in the below sections.

2.5.1. Determination of pH_{zpc}

To determine the pH_{zpc}, first, the pH of the initial solution was adjusted between 2 and 12 by 1 M NaOH and HCl solutions. Then 0.25 g of the magnetic $NiFe_2O_4$ nanocomposite was added to Erlenmeyer flasks containing 50 mL of distilled water. After 24 h, the samples were taken from the shaker, and their pH was measured again. The graph of the initial pH was plotted against the final pH. The intersection point of the two curves was introduced as pH_{zpc}.

2.5.2. Adsorption experiments

In this study, all chemicals were obtained from Merck, Germany. Penicillin G powder was purchased from Sigma Aldrich and used to prepare a stock solution of 500 mg/L. The other concentrations of penicillin G were prepared by diluting the stock solution. In this research, the effects of parameters such as pH (3, 5, 7, 9, 11), magnetic $NiFe_2O_4$ nanocomposite dosages (0.03, 0.5, 1, 1.5, and 2 g/L), initial concentration of penicillin G (2, 5, 10, 15, 20, and 30 mg/L), contact time (5, 15, 20, 40, 60, 90 min), and temperature (283–313 K) were evaluated on penicillin G adsorption by the $NiFe_2O_4$ magnetic nanocomposite. HCl and NaOH solutions were used to adjust the pH. A shaker (Multi shaker, NB-101MT, Korea) was used to mix the sample. Then, the nanocomposite was separated by an external magnet and centrifuged after passing through a 0.45-μm Whatman filter paper (Sigma-301, Germany). Next, the concentration of penicillin G residue was determined by a UV-Visible spectrophotometer (UV/Vis Spectrophotometer T80+, instrument) at a wavelength of 290 nm (Kamranifar *et al.* 2019a). Then, the adsorption capacity, kinetics, isotherms, and thermodynamics of the penicillin G adsorption process on the magnetic nanocomposite $NiFe_2O_4$ were determined. The amount of penicillin G adsorbed on the magnetic $NiFe_2O_4$ nanocomposite was calculated using the following equation:

$$q = \frac{(C_0 - C_e)V}{m} \tag{1}$$

where q is the amount of penicillin G adsorbed by $NiFe_2O_4$ (mg/g); C_0 is the initial penicillin G concentration (mg/L); C_e is the equilibrium concentration of penicillin G (mg/L); V is the initial solution volume (L); and m is the magnetic $NiFe_2O_4$ nanocomposite dosage (Naghizadeh *et al.* 2013b).

3. RESULTS AND DISCUSSION

3.1. Characteristics of adsorbent

3.1.1. XRD analysis

The purity and phase of the as-fabricated samples were characterized by XRD. Prepared magnetic $NiFe_2O_4$ nanocomposites were subjected to XRD and as can be seen in Figure 2, the considered diffraction peaks with 2θ values of 30.43°, 36.12°, 37.19°, 43.27°, 54.63°, 57.18°, and 63.84° are related to the planes (2 2 0), (3 1 1), (2 2 2), (4 0 0), (4 2 2), (5 1 1), and (4 4 0) of crystalline nickel ferrite, respectively. No additional phases were identified. Planes of the cubic spinel ferrite are matched with JCPDS Card No. 01-074-2081. The crystalline phase and diffraction information of the synthesized magnetic $NiFe_2O_4$ nanocomposite were consistent with previous studies (Sivakumar *et al.* 2012).

3.1.2. FESEM and energy-dispersive spectroscopy (EDS)-mapping analyses

To investigate the morphology and particle size of the magnetic magnetic $NiFe_2O_4$ nanocomposite, FESEM measurements were performed. The scanning electron micrograph of the synthesized magnetic $NiFe_2O_4$ nanocomposite with the elemental mapping using EDS is shown in Figure 3. As can be seen, the particle size is regular and the larger particles may be owing to the agglomeration of small magnetic particles. By carefully examining Figure 3, it can be seen that the magnetic $NiFe_2O_4$ nanocomposite is spherical-like in morphology with a size of approximately 50–70 nm. EDS-mapping spectra of the magnetic

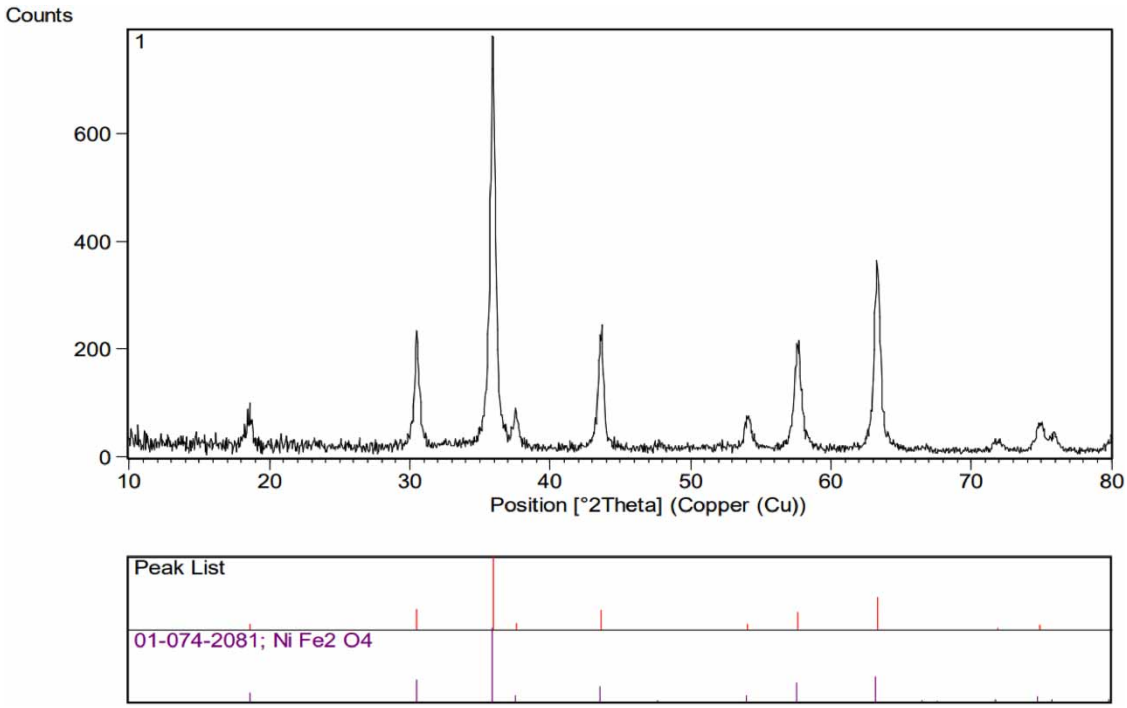

Figure 2 | XRD pattern of the $NiFe_2O_4$ nanocomposite.

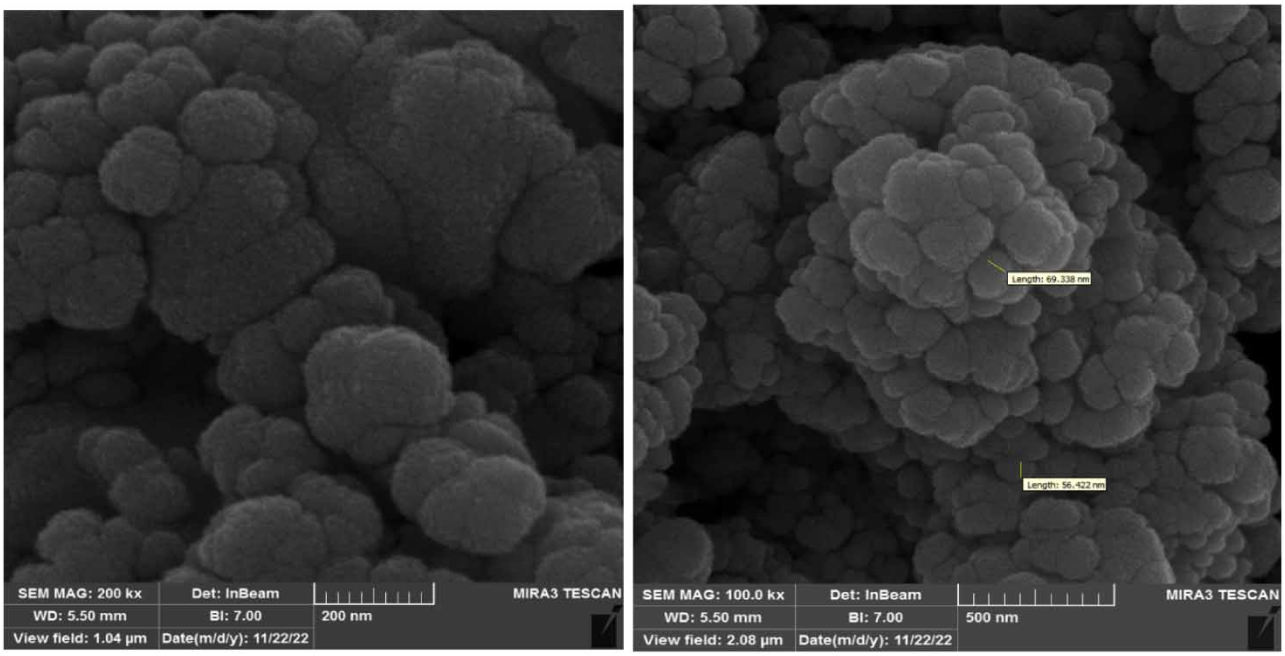

Figure 3 | FESEM spectra images of the $NiFe_2O_4$ nanocomposite.

$NiFe_2O_4$ nanocomposite are shown in Figures 4 and 5. As can be seen, the EDS spectrum and elemental mappings of the magnetic $NiFe_2O_4$ nanocomposite illustrate the presence and the uniform distribution of nickel (Ni), iron (Fe), and oxygen (O) elements, which confirm the synthesis of magnetic $NiFe_2O_4$ nanocomposite. The results of this analysis agreed with the results reported by Vivekanandhan *et al.* (2013).

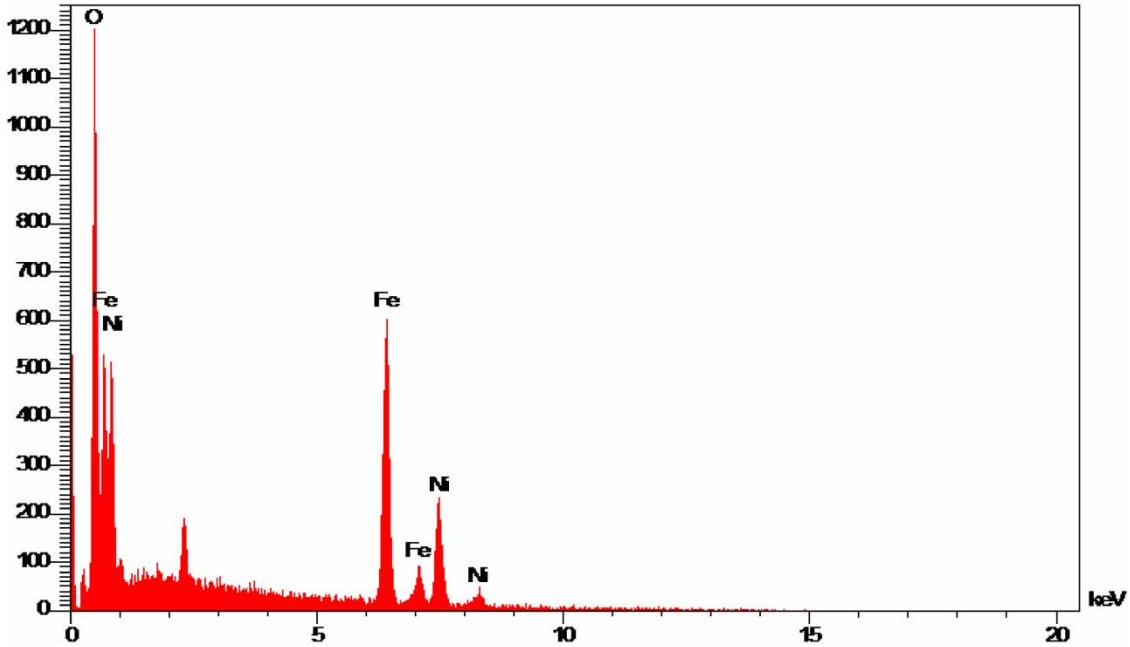

Figure 4 | EDX curve of the magnetic $NiFe_2O_4$ nanocomposite.

3.1.3. FTIR analysis

FTIR was used for the identification of functional group presence in the samples. Structural coordination of the magnetic $NiFe_2O_4$ nanocomposite was studied using FTIR analysis, and the recorded spectrum is shown in Figure 6. By examining the UV spectrum, two bands at 3,458 and 1,643 cm^{-1} were assigned to the typical stretching modes of absorbed water (H_2O). There are two significant peaks in the area below 1,000 cm^{-1}. The peaks at 496 and 674 cm^{-1} are related to the octahedral (Fe^{3+}-O) and tetrahedral (Ni^{2+}/Fe^{3+}-O) frameworks of Fe or Ni ions, respectively (Shirzadi-Ahodashti *et al.* 2020). Therefore, this FTIR spectrum proves that a magnetic $NiFe_2O_4$ nanocomposite was formed.

3.1.4. VSM analysis

VSM analysis is the main method to study the magnetic properties of materials. The result of this analysis is to obtain the hysteresis curve or the hysteresis loop of the material, and using it, data such as saturation magnetization, inhibition, and magnetic permeability can be calculated. The results of VSM analysis of magnetic $NiFe_2O_4$ nanocomposite are shown in Figure 7. As can be seen in the graph, the magnetic property of these nanoparticles is about 25 emu/g, which shows that the nanoparticles have magnetic properties and are easily separated and recovered by an external magnet.

3.2. UV–Vis absorption spectra of penicillin G

UV–Vis spectroscopic analysis is a basic test for measuring absorption wavelengths, identifying compounds, measuring band gaps, and monitoring reaction progress (Mortazavi-Derazkola *et al.* 2021a, 2021b). In this study, the optimal wavelength for measuring different concentrations of penicillin G was obtained using the UV–Vis spectrum. According to Figure 8, the intensity of: Intense Surface Plasmon Resonance (SPR) bands increased with increasing the concentration of penicillin G in the solution. The absorbance of the samples was read in the range of 200–400 nm with a spectrophotometer and it was observed that the maximum absorption of penicillin G in all studied concentrations was at the wavelength of 290 nm.

3.3. pH_{zpc} determination

pH_{zpc} is the point where the positive and negative electric charges on the surface of the adsorbent reach equilibrium and the surface charge of the adsorbent is neutral (Derakhshani *et al.* 2023a). Figure 9 shows that the pH_{zpc} of the magnetic $NiFe_2O_4$ nanocomposite is about 6.9. Therefore, at a pH higher than 6.9, the adsorbent surface has a negative charge, and at a pH lower than 6.8, the adsorbent surface has a positive charge.

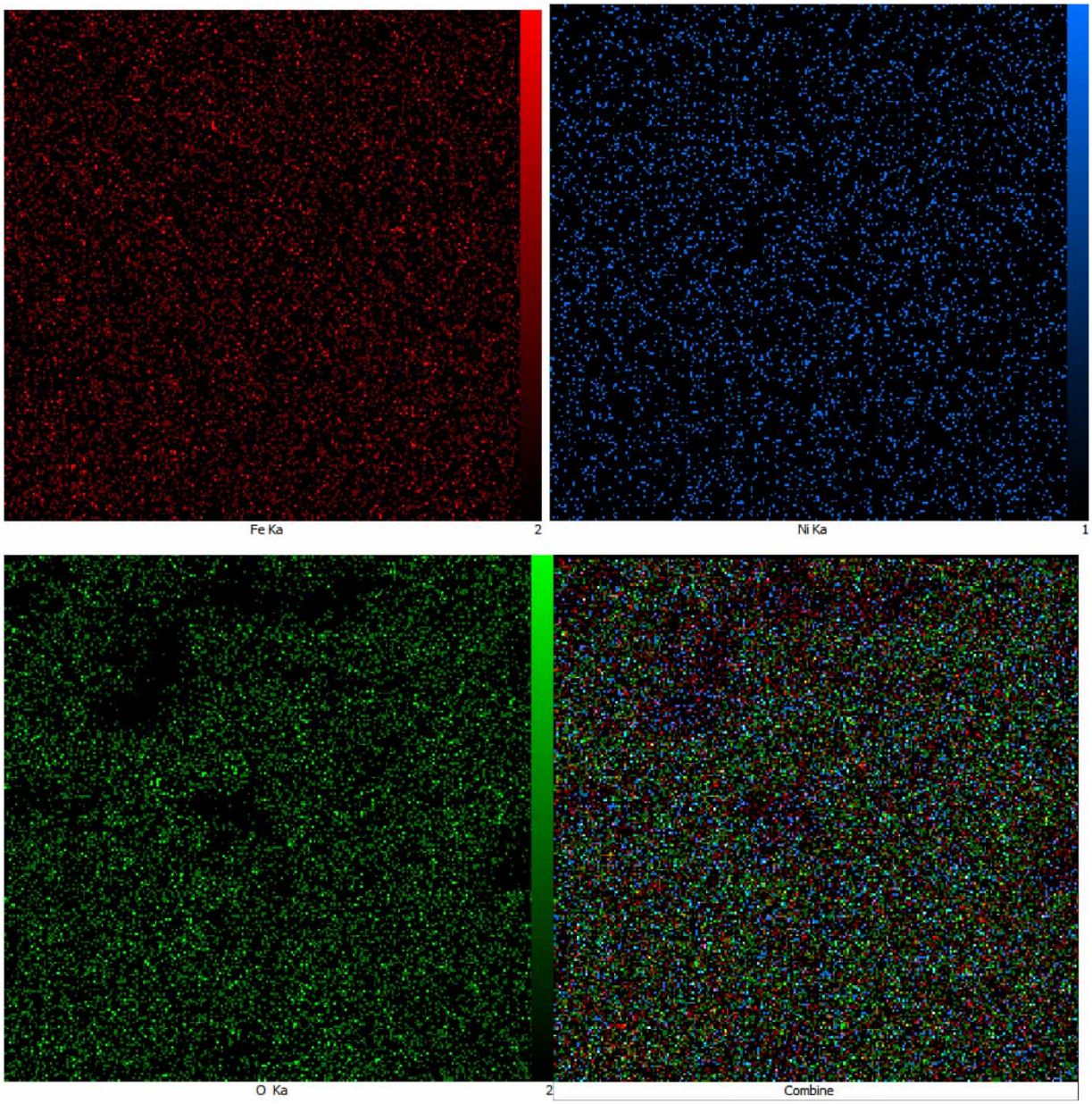

Figure 5 | Mapping spectra of the magnetic $NiFe_2O_4$ nanocomposite.

3.4. Influence of solution pH

In this study, the effect of solution pH with values of 3, 5, 7, 9, and 11 on the adsorption of penicillin G by the magnetic $NiFe_2O_4$ nanocomposite was investigated and the results are shown in Figure 10. The results of this diagram show that the highest adsorption percentage of penicillin G by the nanocomposite occurred at pH 9.

As pH increased from 3 to 9, the adsorption capacity of penicillin G increased from 2.93 to 12.40 mg/g. The pH of the solution is one of the important parameters in the process of penicillin G surface adsorption on the adsorbent because it has a great effect on the efficiency of the adsorption process and changes in the pH of the solution cause a change in the surface charge of the adsorbent (Samarghandi *et al.* 2015; Mousavi *et al.* 2021). The increase in the adsorption of penicillin G in the alkaline solution pH ($pH > pH_{pzc}$) can be related to the negative charge on the surface of $NiFe_2O_4$ nanocomposite and the activation of electrostatic attraction between penicillin G and the nanocomposite for adsorption.

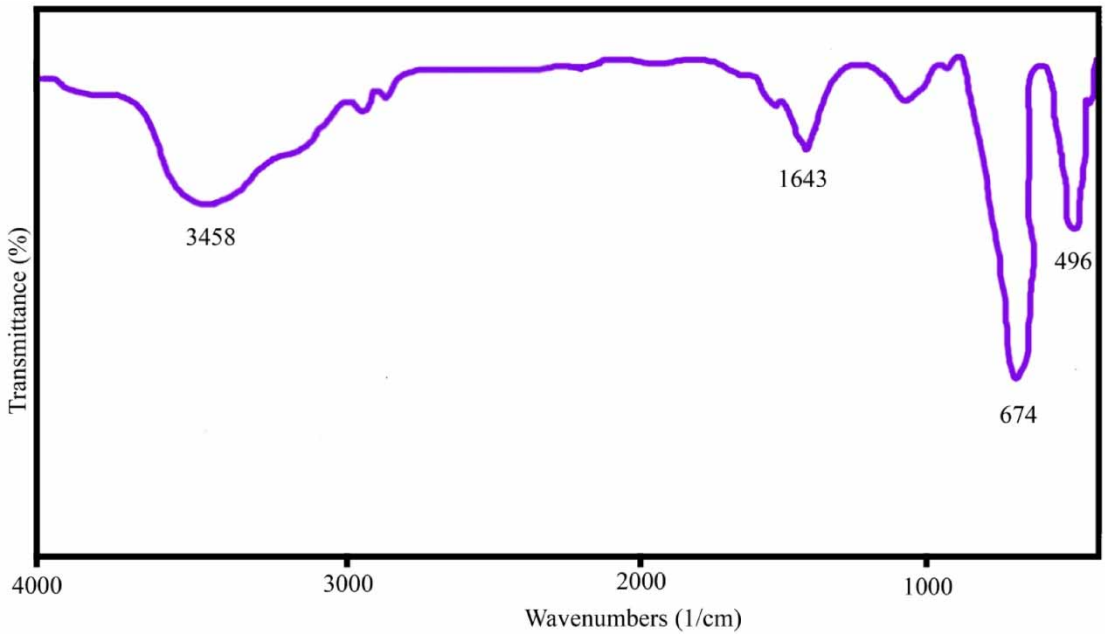

Figure 6 | FTIR analysis of the magnetic $NiFe_2O_4$ nanocomposite.

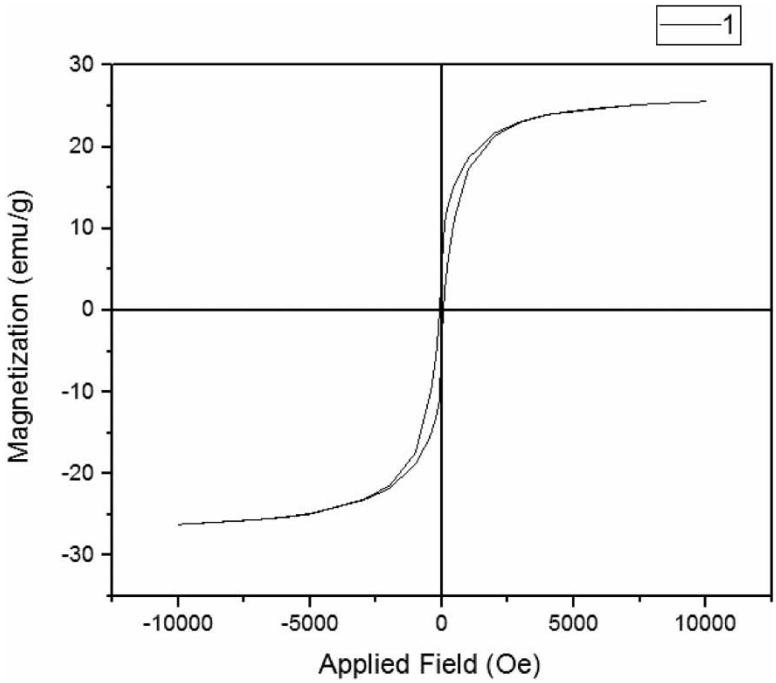

Figure 7 | VSM analysis of the magnetic $NiFe_2O_4$ nanocomposite.

The decrease in the adsorption of penicillin G at acidic pH is due to the increase in the repulsive force between penicillin G and the adsorbent. In the study conducted in 2019 by Nourmradi *et al.*, the removal of penicillin G by modified cationic surfactant montmorillonite was investigated and similar results were obtained. Their findings showed that for the removal of penicillin G, the adsorption capacity of the modified clay was 88.5 mg/g at a contact time of 60 min at pH 9 (Nourmoradi *et al.* 2019).

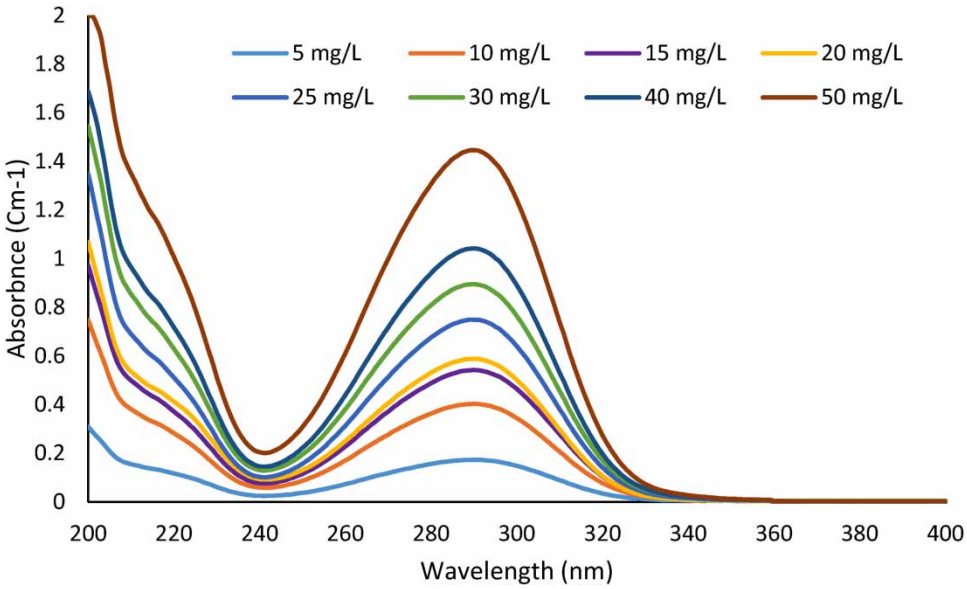

Figure 8 | UV–Vis absorption spectra of penicillin G at room temperature and different penicillin G concentrations.

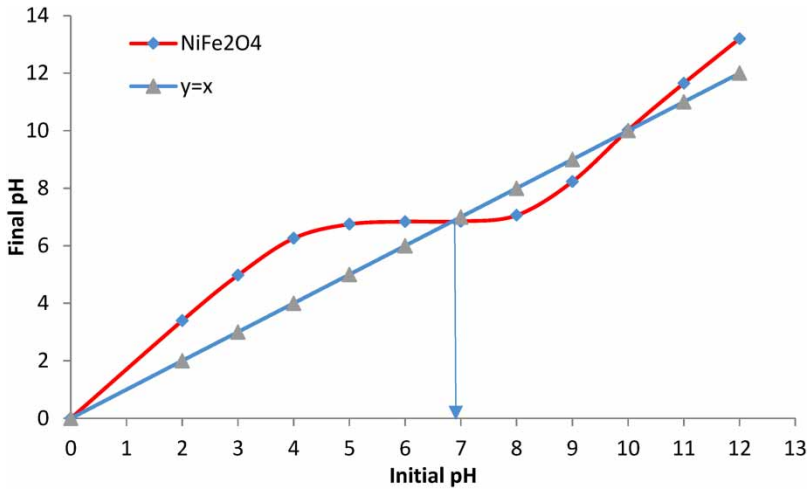

Figure 9 | pH_{zpc} of magnetic NiF_2O_4 nanocomposite.

3.5. Influence of adsorbent dosage

In this study, the effect of adsorbent dose (0.3, 0.5, 1, 1.5, and 2 g/L) on the adsorption of penicillin G by the magnetic $NiFe_2O_4$ nanocomposite was investigated, and the results are shown in Figure 11.

As it is clear from Figure 11, with the increase in adsorbent dosage, the percentage of adsorption increases somewhat. By increasing the amount of adsorbent, the surface area and the number of accessible places for surface adsorption of the pollutant also increase (Ahmadian 2013). However, with a further increase in the adsorbent dose, the number of active sites of adsorbent becomes much higher than the threshold points. Therefore, only a part of the active sites of adsorbent is occupied by penicillin G, and as a result, the adsorption capacity decreases (Wu *et al.* 2013a). On the other hand, according to the $q = ((C_0 – C_e)\ v)/m$ formula, the denominator of the fraction increases with the increase in the adsorbent dose, but the rest of the parameters are constant; therefore, the adsorption capacity of penicillin G decreases.

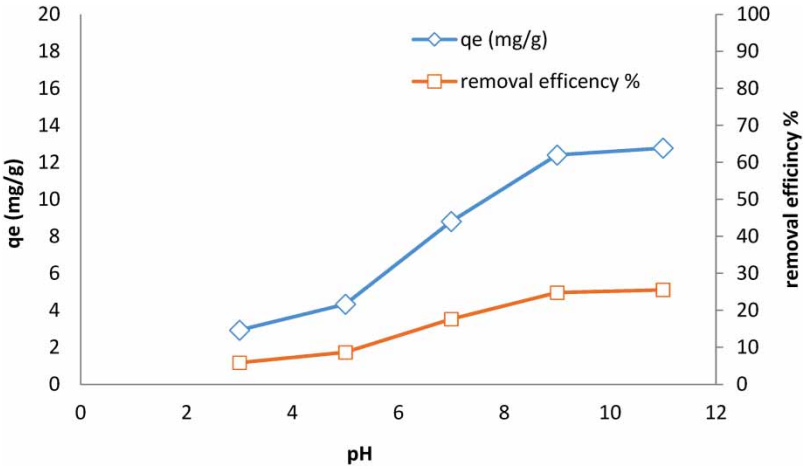

Figure 10 | Influence of pH for the adsorption of penicillin G by the magnetic $NiFe_2O_4$ nanocomposite.

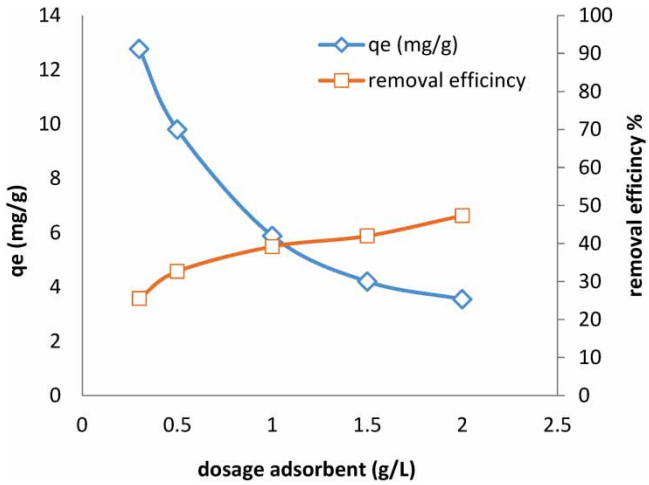

Figure 11 | Influence of adsorbent dosage for the adsorption of penicillin G by the magnetic $NiFe_2O_4$ nanocomposite.

3.6. Influence of contact time and initial concentration of penicillin G

The initial concentration of penicillin G is one of the most important parameters that affect its adsorption by the magnetic $NiFe_2O_4$ nanocomposite. In this study, the effect of contact time (10–90 min) and initial concentration of penicillin G (2, 5, 10, 15, 20, and 30 mg/L) on its adsorption by the adsorbent nanocomposite were investigated, and the results are shown in Figure 12.

As can be seen from Figure 12, as the concentration of penicillin G increases, the adsorption capacity increases and the maximum adsorption capacity occurs in 20 min. The reason is that in the initial stage, a large number of active sites on the adsorbent are available and the high driving force causes the rapid transfer of penicillin G molecules to the surface of absorbent nanoparticles. After that, the adsorption capacity gradually decreases and then reaches equilibrium. The decrease in the adsorption rate is due to the decrease in the number of active sites remaining on the adsorbent (Naghizadeh *et al.* 2013b; Wu *et al.* 2013b; Mohammadi *et al.* 2022). The reason for increasing the adsorption capacity by increasing the concentration of penicillin G is that increasing the initial concentration leads to an increase in the probability of contact between the pollutant and the adsorbent, and finally, the active sites of adsorption are used to the maximum (Balarak *et al.* 2017; Akbari *et al.* 2019).

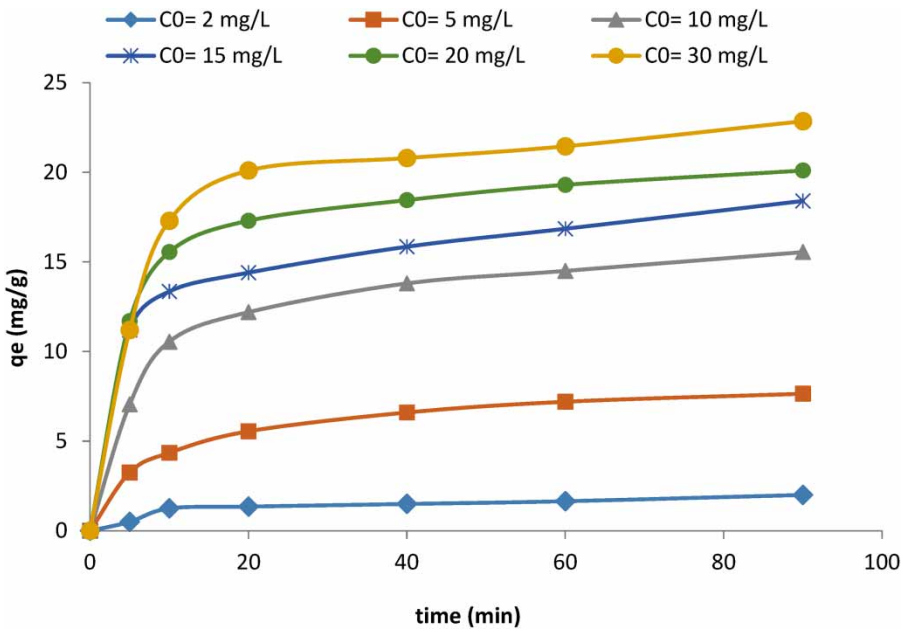

Figure 12 | Influence of contact time and initial concentration for the adsorption of penicillin G by the magnetic $NiFe_2O_4$ nanocomposite.

3.7. Influence of the temperature and the thermodynamic process

To determine the effect of temperature on the adsorption process of penicillin G by $NiFe_2O_4$ magnetic nanoparticles, temperatures of 283, 293, 303, and 313 K were selected. The adsorption process was carried out at pH 9, a nanoparticle dose of 0.3 g/L, and the penicillin G concentration of 15 mg/L for 20 min. As can be seen from Figure 13, the adsorption capacity of magnetic nanoparticles increases with increasing temperature, and this may be because the inactive sites on the surface of the adsorbent become active with increasing temperature (Gerçel & Gerçel 2007; Hossein Panahi *et al.* 2020). All the thermodynamic parameters were determined from the following equations (Naghizadeh *et al.* 2017b):

$$K_c = \frac{C_{\mathrm{Ad}}}{C_e} \tag{2}$$

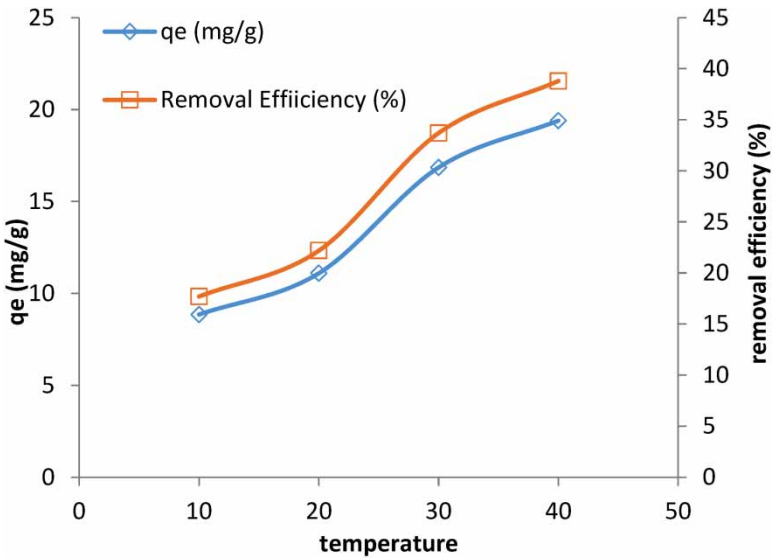

Figure 13 | Influence of temperature for the adsorption of penicillin G by the magnetic $NiFe_2O_4$ nanocomposite.

$$\Delta G = -\mathrm{RT}\ln K_c \tag{3}$$

$$\ln K_c = \frac{\Delta S}{R} - \frac{\Delta H}{\mathrm{RT}} \tag{4}$$

where K_c is the equilibrium constant, C_{Ad} is the concentration of penicillin G adsorbed on $NiFe_2O_4$ at equilibrium (mg/L), C_e is the equilibrium concentration of penicillin G in the solution (mg/L), R is the gas constant (8.314 J/(K·mol)), and T is the temperature in Kelvin. The values of $\Delta H°$ and $\Delta S°$ can be obtained from the slope and intercept of the Van't Hoff plot of ln K_c versus $1/T$.

Table 1 shows the thermodynamic parameters of the adsorption process including enthalpy changes (ΔH), entropy changes (ΔS), and Gibbs free-energy changes (ΔG). In this table, it is shown that ΔH and ΔS are positive and ΔG is negative. The positive value of ΔH indicates that the adsorption process of penicillin G by nanoparticles is naturally endothermic and the adsorption capacity of the adsorbent increases with increasing temperature. According to the results of Table 2, ΔG has negative values, and this indicates the possibility of the spontaneous adsorption process. That is, the adsorption process can be done without the need to add energy from the outside.

3.8. Determination of adsorption kinetics

Reaction kinetics is used to predict the adsorption rate of the pollutants. In this study, pseudo-first-order and pseudo-second-order kinetic models were evaluated for penicillin G adsorption on the magnetic $NiFe_2O_4$ nanocomposite, and the results are shown in Figure 14 and Table 2.

By investigating the correlation coefficient obtained for the pseudo-first-order and pseudo-second-order kinetic models, it was found that the adsorption data in this research follow the pseudo-second-order kinetic model. By examining and comparing the value of q_e in experimental and kinetic models, we conclude that the experimental data are much closer to the pseudo-second-order model data than to the pseudo-first-order model.

3.9. Study of adsorption isotherm models

Five models, namely Langmuir, Freundlich, Brunauer -Emmett -Teller (BET), Temkin, and Dubinin-Radushkevich, were used to investigate the adsorption isotherms of penicillin G by $NiFe_2O_4$ magnetic nanoparticles, and their data are presented in Table 3.

Table 1 | Thermodynamics parameters of penicillin G adsorption by the magnetic $NiFe_2O_4$ nanocomposite

			Thermodynamics parameters		
Adsorbent	**T (K)**	**q_e (mg/g)**	**ΔG (kJ/mol)**	**ΔH (kJ/mol)**	**ΔS (J/mol K)**
$NiFe_2O_4$	283	8.85	−0.17	28.14	99.81
	293	11.1	−0.87		
	303	16.85	−2.35		
	313	19.4	−3.00		

Table 2 | Kinetics constant calculations for the adsorption of penicillin G by the magnetic $NiFe_2O_4$ nanocomposite

		Pseudo-first-order			Pseudo-second-order			
Adsorbent	**C_0 (mg/L)**	**K_1 (min^{-1})**	**q_e, cal (mg/g)**	**R^2**	**K_2 (g/mg min)**	**q_e, cal (mg/g)**	**R^2**	**q_e, exp (mg/g)**
$NiFe_2O_4$	2.00	0.025	1.34	0.88	0.05	2.06	0.964	2.10
	5.00	0.034	3.36	0.78	0.02	8.00	0.991	7.75
	10.00	0.036	5.14	0.65	0.01	15.97	0.994	15.65
	15.00	0.033	5.31	0.58	0.01	18.50	0.994	18.50
	20.00	0.036	4.80	0.68	0.02	20.42	0.998	20.20
	30.00	0.035	5.63	0.60	0.01	23.22	0.996	22.95

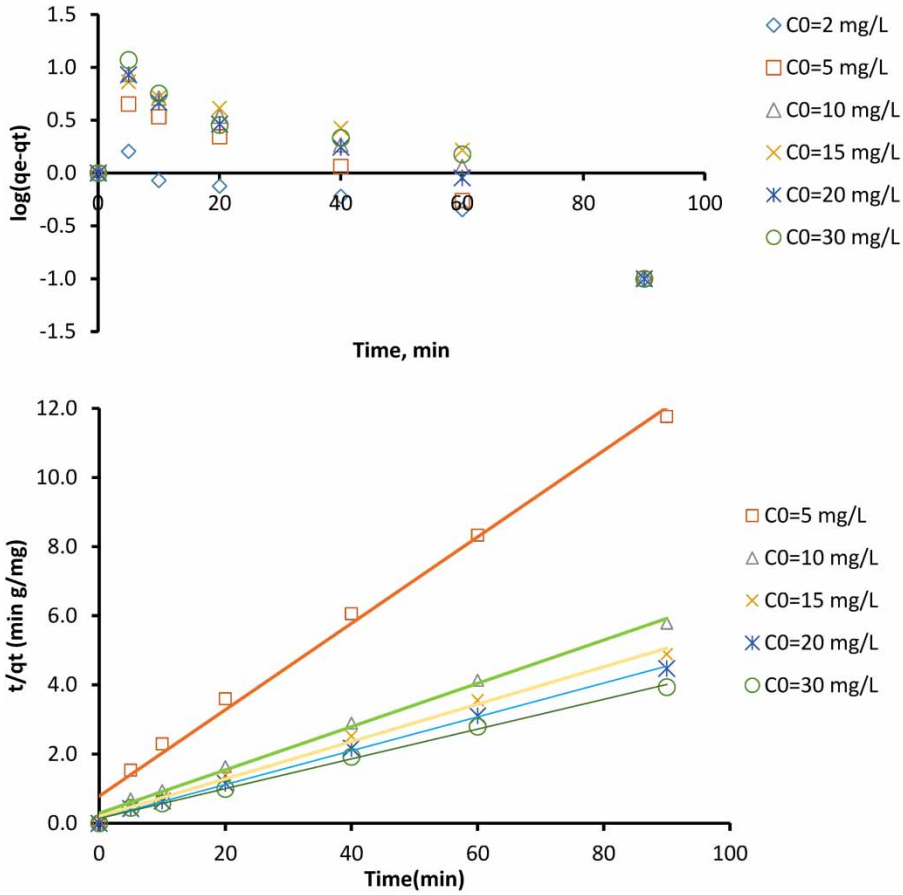

Figure 14 | Pseudo-first-order kinetics and pseudo-second-order kinetics of penicillin G adsorption by the magnetic $NiFe_2O_4$ nanocomposite.

Table 3 | Isotherm and constant calculations for the adsorption of penicillin G by the magnetic $NiFe_2O_4$ nanocomposite

Isotherms	Constants	Values
Langmuir	q_{max} (mg/g)	13.92
	K_L (L/mg)	0.05
	R_L	0.33
	R^2	0.96
Freundlich	k_f (mg/g)	0.94
	$1/n$	1.12
	N	0.89
	R^2	0.94
BET	$1/A{\cdot}Xm$	26.87
	$(A-1)/(A{\cdot}Xm)$	34.84
	A	937.04
	Xm	26.90
	R^2	0.57
Temkin	A_T, L/mg	0.65
	b_T	345.30
	B	7.18
	R^2	0.99
Dubinin-Radushkevich	β, mol^2/kJ^2	0.00
	E, kJ/mol	0.51
	q_m, mg/g	14.64
	R^2	0.96

The comparison of correlation coefficients in Table 3 revealed that the adsorption of penicillin G by the magnetic $NiFe_2O_4$ nanocomposite follows the Temkin isotherm with $R^2 = 0.99$. Adsorption isotherm is one of the most important parameters in the design of pollutant adsorption systems from aqueous solutions, which expresses the interaction between the adsorbent and the adsorbed material. For this reason, it is very important to investigate the adsorption isotherms to optimize the consumption of an adsorbent material and determine its capacity (Piccin *et al.* 2011). As we have seen in this study, the adsorption process of penicillin G follows the Temkin isotherm. In this isotherm, the amount of adsorbed substance is proportional to the logarithm of the adsorbed pressure. This model assumes that the heat of adsorption of all molecules reduces linearly instead of logarithmically with an increasing surface coverage of the adsorbent (Khaled *et al.* 2009; Piccin *et al.* 2011). The Temkin isotherm is obtained by the following equations:

$$q_e = \frac{\mathrm{RT}}{b_T} \ln (A_T C_e) \tag{5}$$

$$B = \frac{\mathrm{RT}}{b_T} \tag{6}$$

$$q_e = B \ \ln A_T + B \ \ln C_e \tag{7}$$

where q_e is the adsorption capacity in equilibrium (mg/g); R is theuniversal gas constant (8.314 J/K mol); T is the temperature (K); b_T is the constant related to heat of sorption (J/mol); A_T is the Temkin isotherm equilibrium binding constant (L/mg); and C_e is the concentration of the solute at equilibrium (mg/L).

The values of A_T, b_T, and B are given in Table 3.

In the study of Kamranifar *et al.* (2019a), who investigated the adsorption of penicillin G by magnetic nanocomposites, they concluded that the adsorption of penicillin G had better compatibility with the Langmuir model and then with Temkin, Freundlich, and Dubinin–Radushkevich models.

4. CONCLUSION

This study was conducted to evaluate the effect of magnetic nanoparticles $NiFe_2O_4$ as an adsorbent in the removal of penicillin G from aqueous solutions. In this research, the results of the analyses performed (FESEM, XRD, FTIR, VSM, and EDS-mapping) showed that the synthesis of the magnetic $NiFe_2O_4$ nanocomposite was successful. The size of the magnetic $NiFe_2O_4$ nanocomposite was determined to be 50–70 nm based on FESEM analysis. The results obtained from this study showed that the $NiFe_2O_4$ magnetic nanocomposite could absorb penicillin G with a high maximum adsorption capacity in the following optimal conditions: pH = 9, nanocomposite dose: 0.3 g/L, penicillin G concentration: 30 g/L, contact time: 20 min, and time temperature: 313 K. Additionally, the results of the thermodynamic study of the adsorption process showed that the values of ΔH and ΔS are positive and ΔG is negative. According to the results of isotherm studies, the experimental data of penicillin G adsorption by the magnetic $NiFe_2O_4$ nanocomposite follow the Temkin model with $R^2 = 0.99$ and pseudo-second-order kinetics with $R^2 = 0.99$. In general, the findings obtained from this study showed that the magnetic $NiFe_2O_4$ nanocomposite has a high efficiency as an adsorbent for the adsorption of penicillin G.

ACKNOWLEDGMENT

We gratefully acknowledge the Research Council of Birjand University of Medical Sciences (Grant Number: 456905) for the financial support.

ETHICAL APPROVAL

This paper was approved as the Ph.D. thesis on the BUMS ethical committee with code IR.BUMS.REC.1401.004.

AUTHORS CONTRIBUTIONS

All authors contributed to the study's conception and design. Material preparation, data collection, and analysis were performed by E.D., A.N., and S.M-D. The first draft of the manuscript was written by E.D. and all authors commented on previous versions of the manuscript. All authors read and approved the final manuscript.

FUNDING

This research project was funded by the Birjand University of Medical Sciences (Grant Number: 456905).

DATA AVAILABILITY STATEMENT

All relevant data are included in the paper or its Supplementary Information.

CONFLICT OF INTEREST

The authors declare there is no conflict.

REFERENCES

Abu-Dief, A. M., Nassar, I. F. & Elsayed, W. H. 2016 Magnetic $NiFe_2O_4$ nanoparticles: Efficient, heterogeneous and reusable catalyst for synthesis of acetylferrocene chalcones and their anti-tumour activity. *Applied Organometallic Chemistry* **30**, 917–923.

Agarwal, H., Kumar, S. V. & Rajeshkumar, S. 2017 A review on green synthesis of zinc oxide nanoparticles – An eco-friendly approach. *Resource Efficient Technologies* **3**, 406–413.

Ahmadian, M. 2013 Adsorption of humic acid from aqueous solution on single-walled carbon nanotubes. *Asian Journal of Chemistry* **25**, 5319–5324.

Akbari, F., Khodadadi, M., Hossein Panahi, A. & Naghizadeh, A. 2019 Synthesis and characteristics of a novel $FeNi_3/SiO_2/TiO_2$ magnetic nanocomposites and its application in adsorption of humic acid from simulated wastewater: Study of isotherms and kinetics. *Environental Science and Pollution Research* **26**, 32385–32396.

Balarak, D., Mostafapour, F. K., Akbari, H. & Joghtaei, A. 2017 Adsorption of amoxicillin antibiotic from pharmaceutical wastewater by activated carbon prepared from *Azolla filiculoides*. Available at SSRN 3955279.

Bound, J. P. & Voulvoulis, N. 2006 Predicted and measured concentrations for selected pharmaceuticals in UK rivers: Implications for risk assessment. *Water Research* **40**, 2885–2892.

Bousquet-Berthelin, C., Chaumont, D. & Stuerga, D. 2008 Flash microwave synthesis of trevorite nanoparticles. *Journal of Solid State Chemistry* **181**, 616–622.

Chaudhuri, M. & Elmolla, E. S. 2008 *Improvement of Biodegradability of Antibiotics Wastewater by Photo Fenton Process*. In: International Conference on Environment 2008 (ICENV 2008), 15–17 December, 2008, Penang, Malaysia.

Choi, K.-J., Kim, S.-G. & Kim, S.-H. 2008 Removal of antibiotics by coagulation and granular activated carbon filtration. *Journal of Hazardous Materials* **151**, 38–43.

Choudhary, V., Vellingiri, K., Thayyil, M. I. & Philip, L. 2021 Removal of antibiotics from aqueous solutions by electrocatalytic degradation. *Environmental Science: Nano* **8**, 1133–1176.

Dehghani, M., Nasseri, S., Ahmadi, M., Samaei, M. R. & Anushiravani, A. 2014 Removal of penicillin G from aqueous phase by Fe^{3+}-TiO_2/UV-A process. *Journal of Environmental Health Science and Engineering* **12**, 56.

Derakhshani, E., Naghizadeh, A., Arabzozani, M. & Frakhondeh, T. 2023a A systematic review of photocatalytic degradation of humic acid in aqueous solution using nanoparticles. *Reviews on Environmental Health* **38** (3), 577–587.

Derakhshani, E., Naghizadeh, A. & Mortazavi-Derazkola, S. 2023b Biosynthesis of $MnFe_2O_4$@TiO_2 magnetic nanocomposite using oleaster tree bark for efficient photocatalytic degradation of humic acid in aqueous solutions. *Environmental Science and Pollution Research* **30** (2), 3862–3871.

El-Shafey, E.-S. I., Al-Lawati, H. & Al-Sumri, A. S. 2012 Ciprofloxacin adsorption from aqueous solution onto chemically prepared carbon from date palm leaflets. *Journal of Environmental Sciences* **24**, 1579–1586.

Fardood, S. T., Atrak, K. & Ramazani, A. 2017 Green synthesis using tragacanth gum and characterization of Ni–Cu–Zn ferrite nanoparticles as a magnetically separable photocatalyst for organic dyes degradation from aqueous solution under visible light. *Journal of Materials Science: Materials in Electronics* **28**, 10739–10746.

Gad-Allah, T. A., Ali, M. E. & Badawy, M. I. 2011 Photocatalytic oxidation of ciprofloxacin under simulated sunlight. *Journal of Hazardous Materials* **186**, 751–755.

Gerçel, Ö. & Gerçel, H. F. 2007 Adsorption of lead (II) ions from aqueous solutions by activated carbon prepared from biomass plant material of *Euphorbia rigida*. *Chemical Engineering Journal* **132**, 289–297.

Githinji, L. J., Musey, M. K. & Ankumah, R. O. 2011 Evaluation of the fate of ciprofloxacin and amoxicillin in domestic wastewater. *Water, Air, & Soil Pollution* **219**, 191–201.

Han, R., Ding, D., Xu, Y., Zou, W., Wang, Y., Li, Y. & Zou, L. 2008 Use of rice husk for the adsorption of Congo red from aqueous solution in column mode. *Bioresource Technology* **99**, 2938–2946.

Hirai, T., Kobayashi, J. & Komasawa, I. 1999 Preparation of acicular ferrite fine particles using an emulsion liquid membrane system. *Langmuir* **15**, 6291–6298.

Hossein Panahi, A., Meshkinian, A., Ashrafi, S. D., Abi, G. & Kamani, H. 2020 Survey of sono-activated persulfate process for treatment of real dairy wastewater. *International Journal of Environmental Science and Technology* **17**, 93–98.

Hussain, I., Singh, N., Singh, A., Singh, H. & Singh, S. 2016 Green synthesis of nanoparticles and its potential application. *Biotechnology Letters* **38**, 545–560.

Iravani, S. 2011 Green synthesis of metal nanoparticles using plants. *Green Chemistry* **13**, 2638–2650.

Kamranifar, M., Allahresani, A. & Naghizadeh, A. 2019a Application of $CoFe_2O_4$@CuS magnetic nanocomposite as a novel adsorbent for removal of penicillin G from aqueous solutions: Isotherm, kinetic and thermodynamic study. *Desalination and Water Treatment* **148**, 363–373.

Kamranifar, M., Allahresani, A. & Naghizadeh, A. 2019b Synthesis and characterizations of a novel $CoFe_2O_4$@CuS magnetic nanocomposite and investigation of its efficiency for photocatalytic degradation of penicillin G antibiotic in simulated wastewater. *Journal of Hazardous Materials* **366**, 545–555.

Khaled, A., El Nemr, A., El-Sikaily, A. & Abdelwahab, O. 2009 Removal of Direct N Blue-106 from artificial textile dye effluent using activated carbon from orange peel: Adsorption isotherm and kinetic studies. *Journal of Hazardous Materials* **165**, 100–110.

Klavarioti, M., Mantzavinos, D. & Kassinos, D. 2009 Removal of residual pharmaceuticals from aqueous systems by advanced oxidation processes. *Environment International* **35**, 402–417.

Kümmerer, K. 2009 Antibiotics in the aquatic environment – A review – Part I. *Chemosphere* **75**, 417–434.

Le-Minh, N., Khan, S., Drewes, J. & Stuetz, R. 2010 Fate of antibiotics during municipal water recycling treatment processes. *Water Research* **44**, 4295–4323.

Li, H., Wu, H.-Z. & Xiao, G.-X. 2010 Effects of synthetic conditions on particle size and magnetic properties of $NiFe_2O_4$. *Powder Technology* **198**, 157–166.

Mohammadi, A. S. & Sardar, M. 2013 The removal of penicillin G from aqueous solutions using chestnut shell modified with H_2SO_4: Isotherm and kinetic study. *Iranian Journal of Health and Environment* **5**, 497–508.

Mohammadi, N., Allahresani, A. & Naghizadeh, A. 2022 Enhanced photo-catalytic degradation of natural organic matters (NOMs) with a novel fibrous silica-copper sulfide nanocomposite (KCC1-CuS). *Journal of Molecular Structure* **1249**, 131624.

Mortazavi-Derazkola, S., Hosseinzadeh, M., Yousefinia, A. & Naghizadeh, A. 2021a Green synthesis and investigation of antibacterial activity of silver nanoparticles using *Eryngium bungei* boiss plant extract. *Journal of Polymers and the Environment* **29**, 2978–2985.

Mortazavi-Derazkola, S., Yousefinia, A., Naghizadeh, A., Lashkari, S. & Hosseinzadeh, M. 2021b Green synthesis and characterization of silver nanoparticles using *Elaeagnus angustifolia* bark extract and study of its antibacterial effect. *Journal of Polymers and the Environment* **29** (11), 3539–3547.

Mousavi, S. A., Kamarehie, B., Almasi, A., Darvishmotevalli, M., Salari, M., Moradnia, M., Azimi, F., Ghaderpoori, M., Neyazi, Z. & Karami, M. A. 2021 Removal of Rhodamine B from aqueous solution by stalk corn activated carbon: Adsorption and kinetic study. *Biomass Conversion and Biorefinery*, 7927–7936.

Naghizadeh, A., Nasseri, S., Mahvi, A. H., Kalantary, R. R. & Rashidi, A. 2013a Continuous adsorption of natural organic matters in a column packed with carbon nanotubes. *Journal of Environmental Health Science and Engineering* **11**, 14.

Naghizadeh, A., Nasseri, S., Rashidi, A., Rezaei Kalantary, R., Nabizadeh, R. & Mahvi, A. 2013b Adsorption kinetics and thermodynamics of hydrophobic natural organic matter (NOM) removal from aqueous solution by multi-wall carbon nanotubes. *Water Science and Technology: Water Supply* **13**, 273–285.

Naghizadeh, A., Momeni, F. & Derakhshani, E. 2017a Efficiency of ultrasonic process in regeneration of graphene nanoparticles saturated with humic acid. *Desalination and Water Treatment* **70**, 290–293.

Naghizadeh, A., Shahabi, H., Derakhshani, E., Ghasemi, F. & Mahvi, A. H. 2017b Synthesis of nanochitosan for the removal of fluoride from aqueous solutions: A study of isotherms, kinetics, and thermodynamics. *Fluoride* **50**, 256–268.

Nourmoradi, H., Daneshfar, A., Mazloomi, S., Bagheri, J. & Barati, S. 2019 Removal of penicillin G from aqueous solutions by a cationic surfactant modified montmorillonite. *MethodsX* **6**, 1967–1973.

Peng, J., Wu, E., Wang, N., Quan, X., Sun, M. & Hu, Q. 2019 Removal of sulfonamide antibiotics from water by adsorption and persulfate oxidation process. *Journal of Molecular Liquids* **274**, 632–638.

Piccin, J., Dotto, G. & Pinto, L. 2011 Adsorption isotherms and thermochemical data of FD&C Red n 40 binding by chitosan. *Brazilian Journal of Chemical Engineering* **28**, 295–304.

Rana, A., Yadav, K. & Jagadevan, S. 2020 A comprehensive review on green synthesis of nature-inspired metal nanoparticles: Mechanism, application and toxicity. *Journal of Cleaner Production* **272**, 122880.

Roy, P., Das, B., Mohanty, A. & Mohapatra, S. 2017 Green synthesis of silver nanoparticles using *Azadirachta indica* leaf extract and its antimicrobial study. *Applied Nanoscience* **7**, 843–850.

Samarghandi, M. R., Al-Musawi, T. J., Mohseni-Bandpi, A. & Zarrabi, M. 2015 Adsorption of cephalexin from aqueous solution using natural zeolite and zeolite coated with manganese oxide nanoparticles. *Journal of Molecular Liquids* **211**, 431–441.

Shirzadi-Ahodashti, M., Ebrahimzadeh, M. A., Amiri, O., Naghizadeh, A. & Mortazavi-Derazkola, S. 2020 Novel NiFe/Si/Au magnetic nanocatalyst: Biogenic synthesis, efficient and reusable catalyst with enhanced visible light photocatalytic degradation and antibacterial activity. *Applied Organometallic Chemistry* **34**, e5467.

Sinsinwar, S., Sarkar, M. K., Suriya, K. R., Nithyanand, P. & Vadivel, V. 2018 Use of agricultural waste (coconut shell) for the synthesis of silver nanoparticles and evaluation of their antibacterial activity against selected human pathogens. *Microbial Pathogenesis* **124**, 30–37.

Sivakumar, P., Ramesh, R., Ramanand, A., Ponnusamy, S. & Muthamizhchelvan, C. 2011a Preparation and properties of nickel ferrite ($NiFe_2O_4$) nanoparticles via sol–gel auto-combustion method. *Materials Research Bulletin* **46**, 2204–2207.

Sivakumar, P., Ramesh, R., Ramanand, A., Ponnusamy, S. & Muthamizhchelvan, C. 2011b Preparation of sheet like polycrystalline $NiFe_2O_4$ nanostructure with PVA matrices and their properties. *Materials Letters* **65**, 1438–1440.

Sivakumar, P., Ramesh, R., Ramanand, A., Ponnusamy, S. & Muthamizhchelvan, C. 2012 Synthesis, studies and growth mechanism of ferromagnetic $NiFe_2O_4$ nanosheet. *Applied Surface Science* **258**, 6648–6652.

Teymourian, H., Salimi, A. & Khezrian, S. 2013 Fe_3O_4 magnetic nanoparticles/reduced graphene oxide nanosheets as a novel electrochemical and bioeletrochemical sensing platform. *Biosensors and Bioelectronics* **49**, 1–8.

Vivekanandhan, S., Venkateswarlu, M., Carnahan, D., Misra, M., Mohanty, A. & Satyanarayana, N. 2013 Sol–gel mediated surface modification of nanocrystalline $NiFe_2O_4$ spinel powders with amorphous SiO_2. *Ceramics International* **39**, 4105–4111.

Wang, T., Pan, X., Ben, W., Wang, J., Hou, P. & Qiang, Z. 2017 Adsorptive removal of antibiotics from water using magnetic ion exchange resin. *Journal of Environmental Sciences* **52**, 111–117.

Wu, S., Zhao, X., Li, Y., Du, Q., Sun, J., Wang, Y., Wang, X., Xia, Y., Wang, Z. & Xia, L. 2013a Adsorption properties of doxorubicin hydrochloride onto graphene oxide: Equilibrium, kinetic and thermodynamic studies. *Materials* **6**, 2026–2042.

Wu, S., Zhao, X., Li, Y., Zhao, C., Du, Q., Sun, J., Wang, Y., Peng, X., Xia, Y. & Wang, Z. 2013b Adsorption of ciprofloxacin onto biocomposite fibers of graphene oxide/calcium alginate. *Chemical Engineering Journal* **230**, 389–395.

Xekoukoulotakis, N. P., Drosou, C., Brebou, C., Chatzisymeon, E., Hapeshi, E., Fatta-Kassinos, D. & Mantzavinos, D. 2011 Kinetics of UV-A/TiO_2 photocatalytic degradation and mineralization of the antibiotic sulfamethoxazole in aqueous matrices. *Catalysis Today* **161**, 163–168.

Xu, W.-H., Zhang, G., Zou, S.-C., Li, X.-D. & Liu, Y.-C. 2007 Determination of selected antibiotics in the Victoria Harbour and the Pearl River, South China using high-performance liquid chromatography-electrospray ionization tandem mass spectrometry. *Environmental Pollution* **145**, 672–679.

Yang, G.-H., Bao, D.-D., Zhang, D.-Q., Wang, C., Qu, L.-L. & Li, H.-T. 2018 Removal of antibiotics from water with an all-carbon 3D nanofiltration membrane. *Nanoscale Research Letters* **13**, 146.

Zandipak, R. & Sobhanardakani, S. 2016 Synthesis of $NiFe_2O_4$ nanoparticles for removal of anionic dyes from aqueous solution. *Desalination and Water Treatment* **57**, 11348–11360.

First received 19 May 2023; accepted in revised form 29 October 2023. Available online 9 November 2023